

# Ti<sub>3</sub>Al PHASE PRECIPITATION DURING VIBRATION FATIGUING FOR A TITANIUM ALLOY<sup>①</sup>

Tao, Chunhu Zhang, Shaoqing Yan, Minggao  
Institute of Aeronautical Materials, Beijing 100095

**ABSTRACT** Ti<sub>3</sub>Al phase was dispersely precipitated in the  $\alpha$  phase during vibration fatiguing for the Widmannstatten, basket-weave and equiaxed structures in a titanium alloy (Ti-6Al-2.5Mo-2Cr-0.5Fe-0.3Si), which leads to decrease the fatigue life. There is a definite orientation relationship between  $\alpha$  and Ti<sub>3</sub>Al:

$$\{0001\}_{\alpha} // \{0001\}_{\text{Ti}_3\text{Al}} \text{ and } \langle 2\bar{1}10 \rangle_{\alpha} // \langle 2\bar{1}10 \rangle_{\text{Ti}_3\text{Al}}$$

**Key words:** vibration fatigue phase precipitation titanium alloy

## 1 INTRODUCTION

Several papers<sup>[1-5]</sup> have reported the effect of microstructures on the vibration fatigue property in titanium alloys; however, these studies concerned only with the fatigue crack initiation and its propagation. The information concerning the phase precipitation in the course of vibration fatiguing has not been reported.

The VT3-1 alloy (Ti-6Al-2.5Mo-2Cr-0.5Fe-0.3Si) is used in aircraft engines as compressor disks and blades, operating at 400 °C. The results on the low cycle fatigue behavior and mechanism of fatigue crack propagation in this alloy were reported<sup>[6, 7]</sup>. Because compressor blades are subjected to strong vibration in service, studying the microstructural stability during vibration is very important. This paper presents the phase precipitation in the course of vibration fatiguing at room temperature and 400 °C in various microstructures for the VT3-1 titanium alloy.

## 2 MATERIALS AND EXPERIMENTAL METHODS

The chemical composition of the VT3-1 alloy is listed in Table 1.

**Table 1 Composition of VT3-1 alloy (wt.-%)**

Al	Mo	Cr	Si	Fe
6.08	2.66	2.01	0.24	0.32
C	N	H	O	Ti
0.018	0.018	0.003	0.09	bal.

The heat treatment procedures in Table 2 were adopted in order to obtain the required microstructures (Widmannstatten, basket-weave, equiaxed and duplex, as shown in Fig. 1). The  $\beta$  transus temperature of the alloy is about 965 °C<sup>[6]</sup>. After the heat treatment mentioned above, the hydrogen content in the alloy reached 0.012 wt.-% and the contents of other elements remained unchanged. Fig. 2

**Table 2 Regimes of rolling and treatment**

Microstructure	Rolling Temp/°C	Heat Treatment
Widmannstatten	940	1 000 °C, 1 h, FC→800 °C, FC*→650 °C, 2 h, AC
Basket-weave	990	920 °C, 1 h, FC→800 °C, FC*→650 °C, 2 h, AC
Equiaxed	940	870 °C, 1 h, FC→800 °C, FC*→650 °C, 2 h, AC
Duplex	940	920 °C, 2 h, AC +550 °C, 6 h, AC

\* with furnace opened.

① Received Sept. 6, 1994

shows the geometry of the vibration fatigue specimen. The fatigue tests were performed on a 5 kW bridge type electromagnetic vibration test machine under stress control, with  $R = -1$ . The vibration frequency was 180 Hz. The alloy foils were observed by H-800 TEM.

### 3 EXPERIMENTAL RESULTS

The foil observation by TEM indicated that there is no precipitation of  $Ti_3Al (\alpha_2)$  phase in all specimens prior to testing. How-

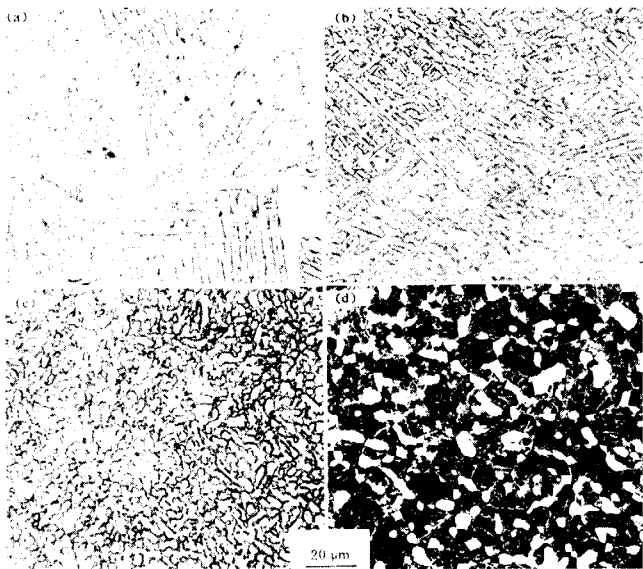


**Fig. 1 Microstructures of the VT3-1 alloy**  
(a)—Widmannstätten; (b)—Basket-weave; (c)—Equiaxed; (d)—Duplex

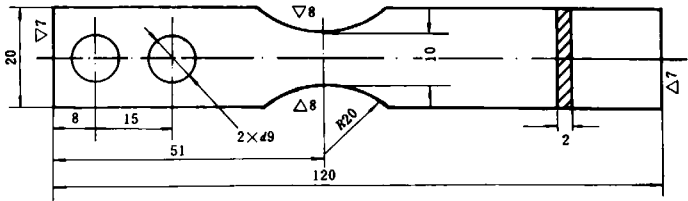


**Fig. 2 Geometry of vibration fatigue specimen**

ever, the Ti<sub>3</sub>Al phase was precipitated (as shown in Fig. 3 and Fig. 4) in the specimens with Widmannstatten, basket-weave or e-quiaxed structures after performing vibration fatigue tests. The TEM dark images, as shown in Fig. 3 and Fig. 4, indicate that Ti<sub>3</sub>Al phases are dispersed in the primary α phase along a common direction. There is a definite orientation relationship between α and the Ti<sub>3</sub>Al<sup>[8]</sup>:

$$\begin{aligned} &(0001)_\alpha // (0001)_{Ti_3Al}, \\ &\langle 2\bar{1}10 \rangle_\alpha // \langle 2\bar{1}10 \rangle_{Ti_3Al} \end{aligned}$$

The length of Ti<sub>3</sub>Al phase particles is in the range of 30~40 nm and the width is ~10 nm. The most precipitation of Ti<sub>3</sub>Al is found in the Widmannstatten structure, with the basket-weave structure having the second largest amount of precipitation. For the specimens with the same structure, there are more Ti<sub>3</sub>Al phase particles in the specimens tested at 400 °C than at room temperature. Also there is no precipitation of Ti<sub>3</sub>Al phase in the specimens with duplex structure after vibration fatigue testing at room temper-

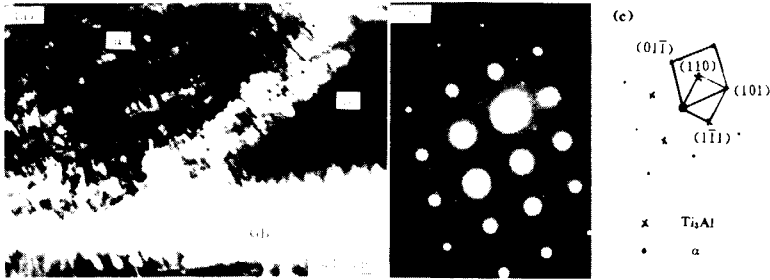


Fig. 3 Ti<sub>3</sub>Al phase precipitation of α- phase for the basket-weave structure  
(a)—Dark field image of Ti<sub>3</sub>Al; (b) Electron diffraction pattern; (c)—Indexing

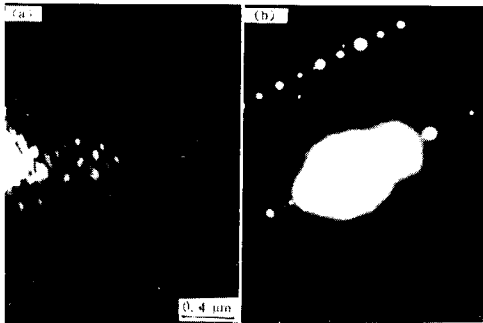


Fig. 4 Dark field image(a) and electron diffraction pattern (b) of Ti<sub>3</sub>Al for the equiaxed structure

ature and 400 °C.

## 4 DISCUSSION

The  $\text{Ti}_3\text{Al}$  phase is liable to be precipitated<sup>[8-10]</sup> in the  $\alpha$  phase during a long term of thermal exposure when the Al equivalent in titanium alloy is more than 9 wt.-%<sup>[11]</sup>. This leads to the friability of alloys.

The Al equivalent is about 8 wt.-% for the VT3-1 titanium alloy. The  $\text{Ti}_3\text{Al}$  phase precipitated in the specimens with Widmannstatten, basket-weave or equiaxed structures after vibration fatigue testing, particularly in the specimens with Widmannstatten structure. It is suggested that this is related to the effect of oxygen and stress: (1) The diffusion rates of the oxygen element are different in the four structures when the specimens were heated in air. On the basis of the diffusion theory and experimental results, the diffusion of the oxygen element in the grain boundary is more rapid by a few orders of magnitude than in the interior of grain. The Widmannstatten structure, composed of coarse  $\text{GB}\alpha$  phase and  $\text{W}\alpha$  platelets, is liable to be polluted by oxygen, which promotes the precipitation of  $\text{Ti}_3\text{Al}$  phase. Therefore, the Widmannstatten structure is associated with the most precipitation of  $\text{Ti}_3\text{Al}$  phase, and the next is the basket-weave structure. (2) Stress promotes a local concentration of Al and O, so the repeated alternating loads lead to an increase of Al equivalent in some regions, which promotes the precipitation of  $\text{Ti}_3\text{Al}$  phase. (3) For the Widmannstatten and basket-weave structures, the slip readily passes through the colonies of  $\text{W}\alpha$  platelets, because of a definite orientation relationship between  $\alpha$  and  $\beta$ <sup>[12]</sup>:

$$\{0001\}_{\alpha} // \{110\}_{\beta} \quad [11\bar{2}0]_{\alpha} // [111]_{\beta} \text{ and } \\ \{00\bar{1}0\}_{\alpha} // \{112\}_{\beta} \quad [11\bar{2}0]_{\alpha} // [111]_{\beta}$$

Consequently, the slip system of  $\alpha$  is parallel to that of  $\beta$ . As a result, the slip has a longer path. At 400 °C in particular, the oxygen easily diffuses into the  $\alpha$  phase along slip paths, which causes a higher content of oxygen in some local regions, consequently promotes precipitation of  $\text{Ti}_3\text{Al}$  phase in these regions.

For the equiaxed structure, the diffusion path of oxygen is short and tortuous, because of its fine grain size and indefinite orientation relationship between  $\alpha$  and  $\beta$ , therefore, the diffusion rate of oxygen was decreased and the  $\text{Ti}_3\text{Al}$  phase precipitated less. In the duplex structure, the content of the primary  $\alpha$  phase is lower; the distance between the  $\alpha$  phase particles is long; and the slip orientation is different. Therefore, the slip path is short and the local concentrations of oxygen and aluminium are limited, so that precipitation of  $\text{Ti}_3\text{Al}$  phase does not take place.

Previous studies<sup>[13]</sup> showed that the long path and planar slip lead to a decrease of fatigue life. The presence of  $\text{Ti}_3\text{Al}$  precipitation phase in the specimens with the Widmannstatten, basket-weave or equiaxed structure favours the localization of slip<sup>[14, 15]</sup>. This induces the piling of dislocations and the stress concentration at phase interfaces. Moreover, when the specimens are suffered from cyclic loading, the repeated planar slip produces dislocation jogs, due to the interaction of the moving dislocations with other dislocations. The dislocations with jogs produce voids when they move<sup>[6]</sup>. From this the fragility and decrease of fatigue life of the alloy rose. Thus, it is reasonable to consider that the shorter fatigue life of the specimens with Widmannstatten<sup>[17]</sup> is associated not only with its lower  $\sigma_b$  but also with the precipitation of  $\text{Ti}_3\text{Al}$  phase during vibration fatiguing.

## 5 CONCLUSION

The  $\text{Ti}_3\text{Al}$  phase precipitated in specimens with Widmannstatten, basket-weave or equiaxed structures during vibration fatiguing, which induced the slip localization and planar slip. Thus, piling dislocations at the phase interfaces is liable to produce the localized stress concentration, which leads to the decrease of fatigue properties.

## REFERENCES

- 1 Gysler, A; Lindigkeit, J; Lutjering, G. In: Proc

- 5th ICSMA, Pergamon Press, 1979.
- 2 Peters, M; Gysler, A; Lutjering, G. AIME, 1980, 1777.
- 3 Stubbington, C A; Bowen, A W. J Mater Sci, 1974, 9: 941.
- 4 Peters, M. Lutjering, G. AIME, 1980, 925.
- 5 Peters, M; Lutjering, G. EPRI CS-2933, 1983.
- 6 Zhang, S Q; Tao, C H; Yan, M G. ASTM STP942, 1988, 838.
- 7 Tao, C H; Zhang, S Q. In: Proc 5th Inter Conf Mech Behavior of Materials, Beijing, 1987.
- 8 Zhang, S Q. Acta Metallurgica Sinica, 1983, 19A (6): 551.
- 9 Welsch, G; Lutjering, G; Gazioglu, K; Bunk, W. Met Trans 1977, 8A: 169.
- 10 Blackburn, M A. Metall Soc AIME, 1967, 239, 1200.
- 11 Rosenberg, H W. The Science, Technology and Application of Titanium. London: Pergamon Press, 1970. 851.
- 12 Margolin, H; Williams, J C; Chesnutt J C; Lutjering, G. In: Proc 4th Inter Conf on Titanium, Kyoto, Japan, 1980.
- 13 Williams J C; Lutering, G. In: Proc 4th Inter Conf on Titanium, Kyoto, Japan, 1980.
- 14 Blackburn, M J; Williams, J C. Trans ASM 1969, 62: 398.
- 15 Lutjering, G; Weissmann, S. Acta Met, 1970, 18: 185.
- 16 Hamajima, T; Lutjering, G; Gerold, V. Acta Met, 1974, 22: 901.
- 17 Tao, C H; Zhang, S Q. J of Aero Mater, 1989, 9(2): 32.

(From page 65)

(3) The characters of the *B*19-*B*19' transformation are: obvious resistivity change, minor heat effect and wide transformation temperature range. *B*19 martensite has higher *E* modulus than the *B*19 martensite and has twin substructure.

#### REFERENCES

- 1 Zhang, Y; Hornbogen, E Z. Metallkde, 1987, 78 (H6): 401.
- 2 Bricknell, R H; Melton, K N; Mercier, O. Met Trans, 1979, 10A: 693.
- 3 Miyazaki, S; Shiotto, I; Otsuka, K; Tamura, H. MRS Int Mtg Adv Mates, 1988, 9: 153.
- 4 Saburi, T; Nenno, S. In: Shanghai Iron and Steel Research Institute(ed), The Proce of The 3rd China-Japan Metal Physics and Physical Metallurgy Symposium, Shanghai: 1988: 61.
- 5 Jin, J L; Zhang, Y; Cai, X X. In: The Proce of the SMM-94 Int Symposium, Beijing: 1994.
- 6 Miyazaki, S; Wayman, C M. Acta Metall, 1988, 36(1): 181.
- 7 Zhang, Y; Ji, Z Q; Gai, G Q. Technical Report of SISRI, 1993, (6): 8.
- 8 Tadaki, T; Wayman, C M. Metallography, 1982, 15: 233, 247.
- 9 Saburi, T; KOMatsu, T; Nenno, S; Watanabe, Y. J of Less-Common Metals. 1986, 118: 217.
- 10 Nam, T H; Saburi, T; Kawamura, Y; Shimizu, K. Materials Trans JIM, 1990, 31: 262.